5-1-1980

Spatial filtering of a projection printer, using partially coherent light

Leon Vlahakes

SPATIAL FILTERING OF A PROJECTION PRINTER USING PARTIALLY COHERENT LIGHT

by

Leon John Vlahakes

A thesis submitted in partial fulfillment
of the requirements for the degree of
Bachelor of Science in the School of
Photographic Arts and Sciences in the
College of Graphic Arts and Photography
of the Rochester Institute of Technology

May, 1980

Signature of the Author.....
Photographic Science
and Instrumentation

Certified by.....
Thesis Adviser

Accepted by.....
Supervisor, Undergraduate Research

SPATIAL FILTERING OF A PROJECTION PRINTER USING PARTIALLY COHERENT LIGHT

by

Leon John Vlahakes

Submitted to the
Photographic Science and Instrumentation Division
in partial fulfillment of the requirements
for the Bachelor of Science degree
at the Rochester Institute of Technology

ABSTRACT

This investigation applied the technique of spatial filtering to a projection printer utilizing partially coherent illumination. The affect of filtering on image quality parameters such as resolution, edge gradient and MTF were determined for a black and white film. Edge gradient analysis was used to derive MTF data from sampled edges. A source diameter of 3 mm and spatial filter diameters of .6, 2.2, and 3.0 mm were used.

Spatial filtering was seen to have a drastic affect on edge gradient and MTF. Increasing the filter diameter resulted in a decrease of cutoff frequency of the system. Spatial filtering had the affect of boosting low frequency modulation by up to 30 percent. Subjectively, however, changes

could not be detected, indicating that the alterations made to the system are not significant to be detected visually. Resolution was found to fluctuate only 15 percent between the application of each filter. Despite gross changes in other imaging characteristics, resolution remained nearly unchanged, indicating that resolution is a poor discriptor of image quality.

ACKNOWLEDGMENTS

Many thanks to John F. Carson of the Photoscience department for his assistance throughout this project. His assistance with mathematical treatments was invaluable. Also, to Richard Norman for fabricating needed equipment.

TABLE OF CONTENTS

LIST OF TABLES

LIST OF FIGURES

INTRODUCTION

The technique of spatial filtering has existed since Ernst Abbe[1] (1893) first applied it to coherent microscope imaging systems. In recent years, it was found that optical image processing, or spatial filtering, could be used for image enhancement and data processing. The periodic nature of image components is broken down into its' Fourier series in a coherent imaging system. This concept is more readily seen in figure 1. At the transform plane, or the conjugate plane to source S, the objective lens resolves a transmission object into its' various Fourier series components. The spatial frequencies denoted as f_{-1} through f_1 indicate the presence of a specific spatial frequency in the object plane, with higher frequency as the distance increases from the optical axis. This investigation is concerned with attenuating the fundamental frequency f_0, and determining its' affect on various image quality parameters.[2]

The concept of spatial filtering must be applied to an optical system utilizing a coherent or partially coherent illuminating geometry. A general overview of cohernece can be demonstrated by Young's experiment, illustrated in figure 2.[3] Choosing a point s' on an extended quasi-monochromatic source of finite width d, it can be seen that a fringe

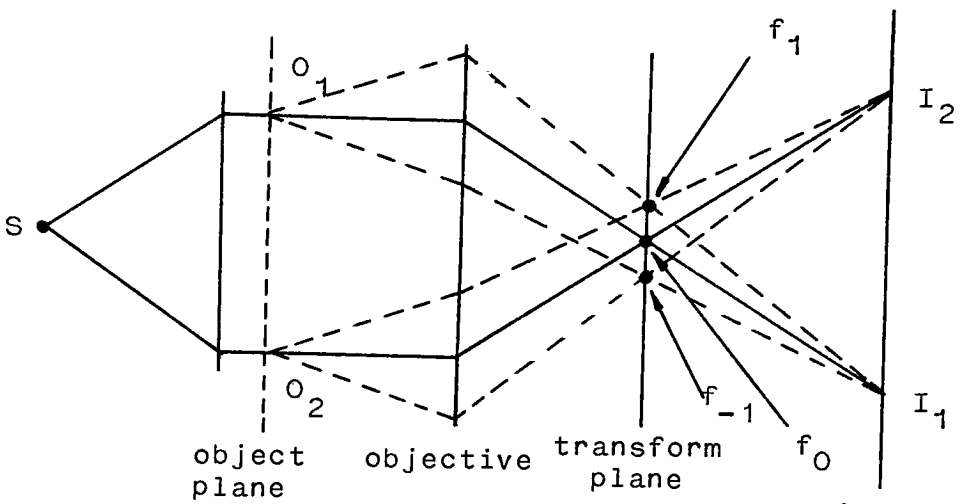

Optical Frequency Spectrum

figure 1

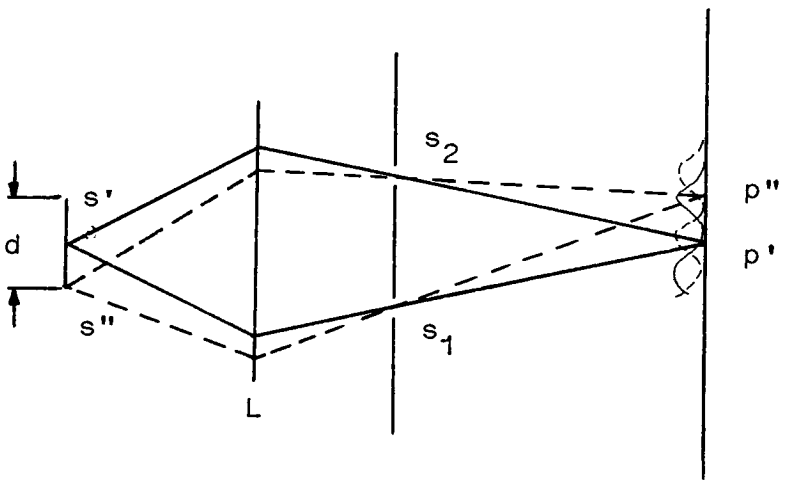

Young's Experiment

figure 2

pattern is generated on the screen after passing through two pinholes, s_1 and s_2, due to an optical path difference. Similarly, source point s" will generate a fringe pattern out of phase with the previous one, as will be true with source points across the source width d. The affect of a finite source size is to produce a superposition of these sinusoidal patterns resulting ia a final sinusoidal wave form of the same frequency, and lower modulation. As the source size d increases, the visibility of these sinusoidal patterns decreases due to a drop in modulation. The degree of coherence for a source is directly related to the visibility of the fringes it produces when used in the geometry shown in figure 2. The fringe visibility is dependent upon: 1) the optical path difference for each source point, which must satisfy the condition that

$$OPD << \frac{\bar{\lambda}^2}{\Delta\bar{\lambda}} \quad ,$$

where $\bar{\lambda}$ = average wavelength
$\Delta\bar{\lambda}$ = bandwidth

which limits the size of the source, and 2)

$$\frac{\Delta\lambda}{\bar{\lambda}} << 1,$$

which limits the spectral output of the illuminating source. If both conditions are satisfied, the illuminating system

will behave as a coherent, quasi-monochromatic source.

In an ideal coherent imaging system arranged in the geometry shown in figure 2, the frequency spectrum present in the transform plane will be represented by a series of delta functions , illustrated in figure 3. The frequency domain

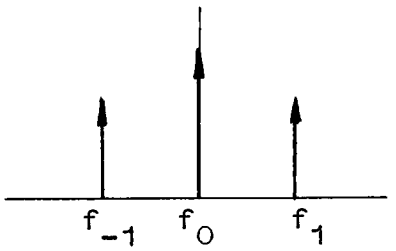

Transform Plane

figure 3

of a transmission object lends itself to filtering at this Fourier transform plane as indicated in figure 4. The

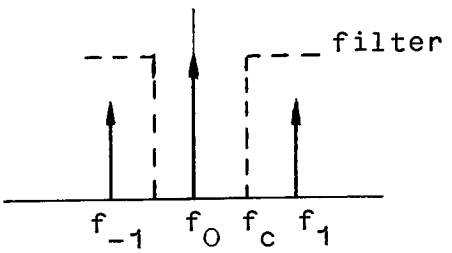

Filtered Fourier Transform

figure 4

dashed line represents a filter having a binary transmission function of zero at the dc frequency value f_0, and one

at all other frequencies. The net result of this filtering is an image with the dc component of the objects Fourier frequency spectrum deleted.

Extending this principle to a finite source size, it can be seen that a superposition of shifted frequency spectra occurs. Figure 5 demonstrates the affect of a finite

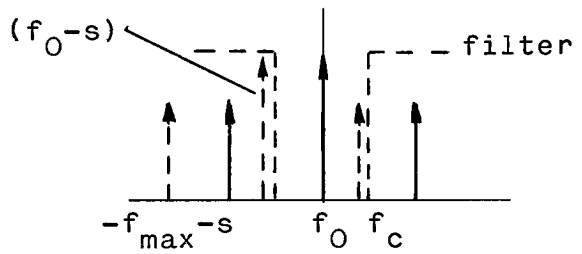

Extended Source Transform

figure 5

source size on the Fourier transform of a transmission object. A source point located at the center of the extended source will produce a frequency spectrum centered about the vertical axis in figure 5, shown with solid lines. Similarly, a source point at the edge of the extended source will produce a frequency spectrum which is shifted by an amount s, shown with dashed lines. It is readily seen that when a binary filter with cutoff frequency f_c is applied to the spectrum, its' affect on the various shifted frequency spectra is different. In the case of figure 5, when the filter is multiplied by the unshifted frequency spectrum,

the dc frequency component f_o is selectively removed. The spectrum shifted by an amount s, is affected quite differently. The function is shifted such that $-f_{max}$-s and f_o-s pass unfiltered, while f_{max}-s is filtered by the binary spatial filter. In the former case, the dc component can be effectively attenuated, while in the latter case, the dc is passed unfiltered. It can be seen that when an extended source is used in an optical system, a spatial filter cannot be effectively applied to the dc component selectively. A superposition of shifted frequency spectra causes other low frequency information to be filtered as well.

A one dimensional mathematical model can be derived to predict the affect of spatial filtering when using an extended source. The illuminating system is assumed to be incoherent, and the affects of diffraction are neglected.

Utilizing a one dimensional sinusoidal object t(x), its' frequency spectrum T(f) may be found by taking its' Fourier transform.

$$t(x) = t_o + mt_o \cos 2\pi f_o x$$

where: t_o= average transmission
f_o= fundamental frequency
m= modulation

In complex terms, the sinusoidal object may be written as

$$t(x) = t_o + \frac{t_o}{2} me^{i2\pi f_o x} + \frac{t_o}{2} me^{-i2\pi f_o x} .$$

In frequency space, the Fourier transform may be expressed as,

$$T(f)=F[t(x)] = t_0\delta(f)+ \frac{t_0}{2}m\delta(f+f_0)+ \frac{t_0}{2}m\delta(f-f_0) \ .$$

A filter function of $tf(nf_0)=tf(f')$ will now be applied to $T(f)$.

$$tf(f')T(f)= t_0\delta(f)tf(f')+ \frac{t_0}{2}mtf(f'+f_0)\delta(f+f_0) + \frac{t_0}{2}mtf(f'-f_0)\delta(f-f_0)$$

Taking the Fourier transform of the filtered frequency spectrum, the filtered object is obtained.

$$t(x)= tf(f') \ F[T(f)] =t_0tf(f')+ \frac{t_0}{2}mtf(f'+f_0)e^{i2\pi f_0x} + \frac{t_0}{2}mtf(f'-f_0)e^{-i2\pi f_0x}$$

Image irradiance is found to be

$$I(x,f',f_0)= |t(x)|^2 = t(x)(t^*(x))$$

$$I(x,f',f_0)= \left[t_0{}^2tf^2(f')+ \frac{t_0}{4}m^2(tf^2(f'+f_0)+tf^2(f'-f_0))\right]$$

dc term

$$+\left[t_0{}^2mtf(f')\cos 2\pi f_0x \ (tf(f'+f_0)+tf(f'-f_0))\right]$$

first harmonic

$$+\left[\frac{t_0}{2}m^2tf(f'-f_0)tf(f'+f_0)\cos 2\pi 2f_0x\right]$$

second harmonic

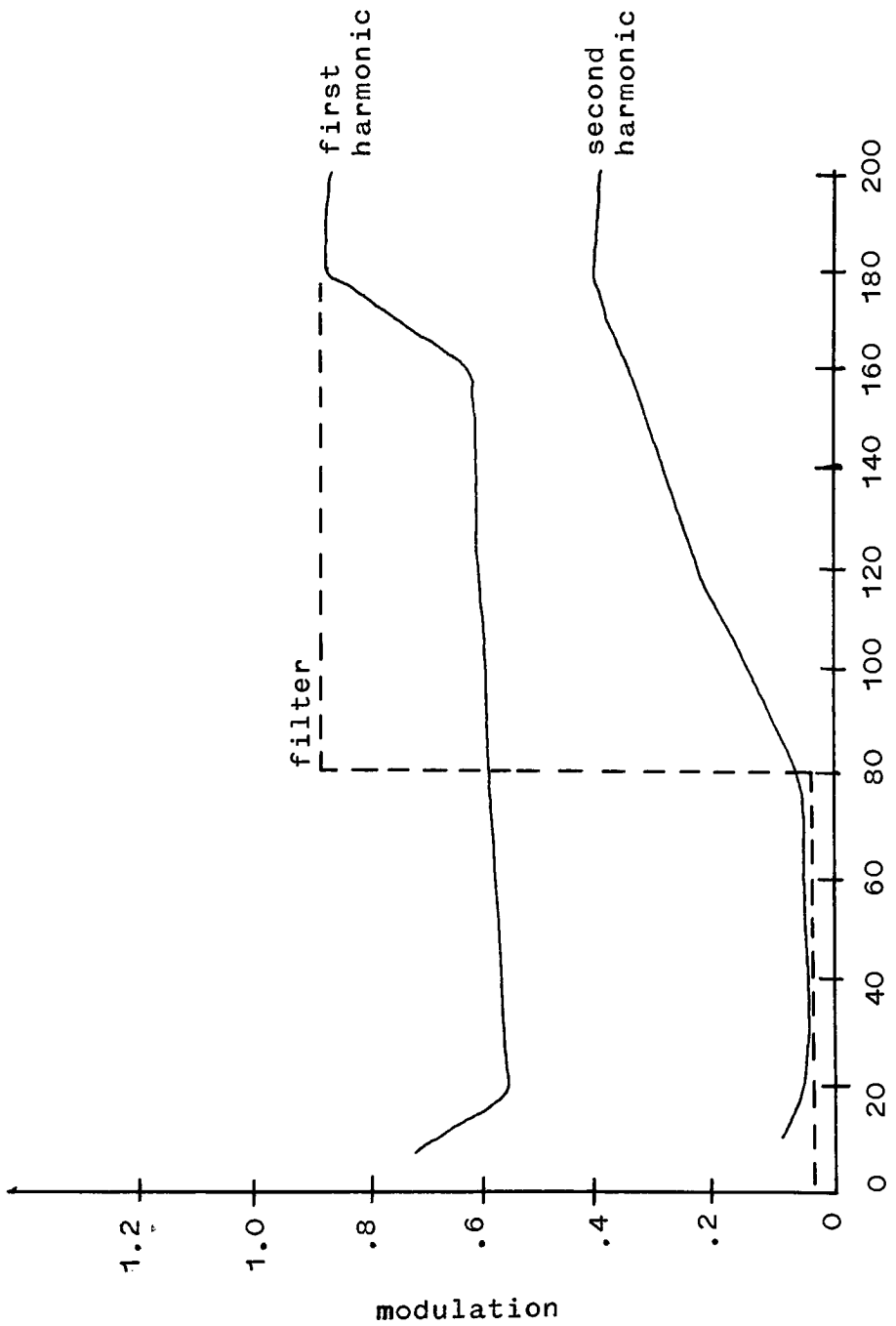

Theoretical Transfer Curves

figure 6

For graphical purposes, let

$$\text{first harmonic modulation} = \frac{\text{first harmonic}}{\text{dc term}}, \text{ and the}$$

$$\text{second harmonic modulation} = \frac{\text{second harmonic}}{\text{dc term}}.$$

Figure 6 illustrates the affect of applying a spatial filter to an incoherent imaging system. Both first harmonic and second harmonic modulation are plotted versus frequency. A filter transmission of .1 was chosen, and object modulation of .5. Frequency units are shown as 0 through 200 with a filter cutoff frequency of 80. It can be seen that at the filter cutoff frequency the second harmonic modulation is beginning to increase, while the filter has a notching affect on the first harmonic modulation. Other models were generated at various filter functions, and it was observed that second harmonic modulation increased with increased filter cutoff frequencies. In terms of image quality, it believed that this increased second harmonic modulation will be observed as "ringing" in edges imaged with the above filtered optical system.

As mentioned previously, spatial filtering must be applied to an optical system having coherent or partially coherent illumination. The degree of coherence for an imaging system has been shown to have a marked affect on image quality parameters such as resolution, and sharpness. The

affect of coherence on two point resolution was investigated by Grimes and Thompson[4]. Their study was based on the separation distance of two point objects necessary to have them resolved in the imaging plane over varied coherence intervals. It was found that resolution increased with incoherent illumination, that is, the separation distance necessary between the two object points decreased with greater incoherence. A more quantitative analysis of the affect of the coherence inter val on image resolution was performed by Radl[5]. Radl concluded that as the degree of coherence of the illuminating source increased, the resolution dropped by a factor of two, until a coherent imaging system was reached. Radl also investigated the affect of coherence on image sharpness. In the same coherence length range examined for resolution, it was illustrated that acutance increased by a factor of three, with increasingly coherent illumination. Prior work by Kinzly[6] yielded similar results when using edge gradient as a criterion. With increasing coherence, the edge gradient was found to increase approximately 25 percent.

The implication of this dependence of resolution and image sharpness on the degree of coherence of the illuminating source at the object plane is that subjective and objective image quality will vary with optical printer geometry and illuminating systems. Past work in the area has shown that a tradeoff exists between resolution and

sharpness as a function of coherence. Increasing the degree of coherence will result in images of higher sharpness, but lower resolution, and vice versa when the degree of coherence is decreased. An optical printer that would maximize resolution and sharpness would prove valuable when attempting to produce high quality images.

It is hypothesized that the technique of spatial frequency filtering applied to an optical printer using a partially coherent illuminating system will exhibit increased sharpness and sinusoidal modulation at a particular optical geometry. The objective of this investigation is to determine the affect of spatial filtering on the image quality parameters described above and apply the math model described to these parameters.

EXPERIMENTAL

The optical configuration used for the experimental work is illustrated in figure 7. A 100 watt mercury arc source was utilized due to its' high power in the blue spectral region. A 436 nm interference filter with a bandpass of 9 nm and a peak transmittance of .5 was used to selectively transmit the mercury line at 435.8 nm. This filter will provide a blue spectral output which corresponds to the sensitivity of many black and white materials. It is assumed that this spectral distribution provides a quasi-monochromatic condition, and therefore the necessary degree of coherence to perform spatial filtering. The converging beam is incident on a double piece of ground glass to produce a totally diffuse source, whose size is determined by an aperture mask, which is labeled effective source. This effective source is located 65 mm from the rear element of the first condenser. A source diameter of 3 mm was chosen to facilitate the manufacturing of spatial filters, to be described later. Using the van Cittert-Zernike theorem, the coherence interval,v, of the 3 mm filtered source may be determined by the expression,

$$v = \frac{3.83 r \lambda}{2\pi a}$$

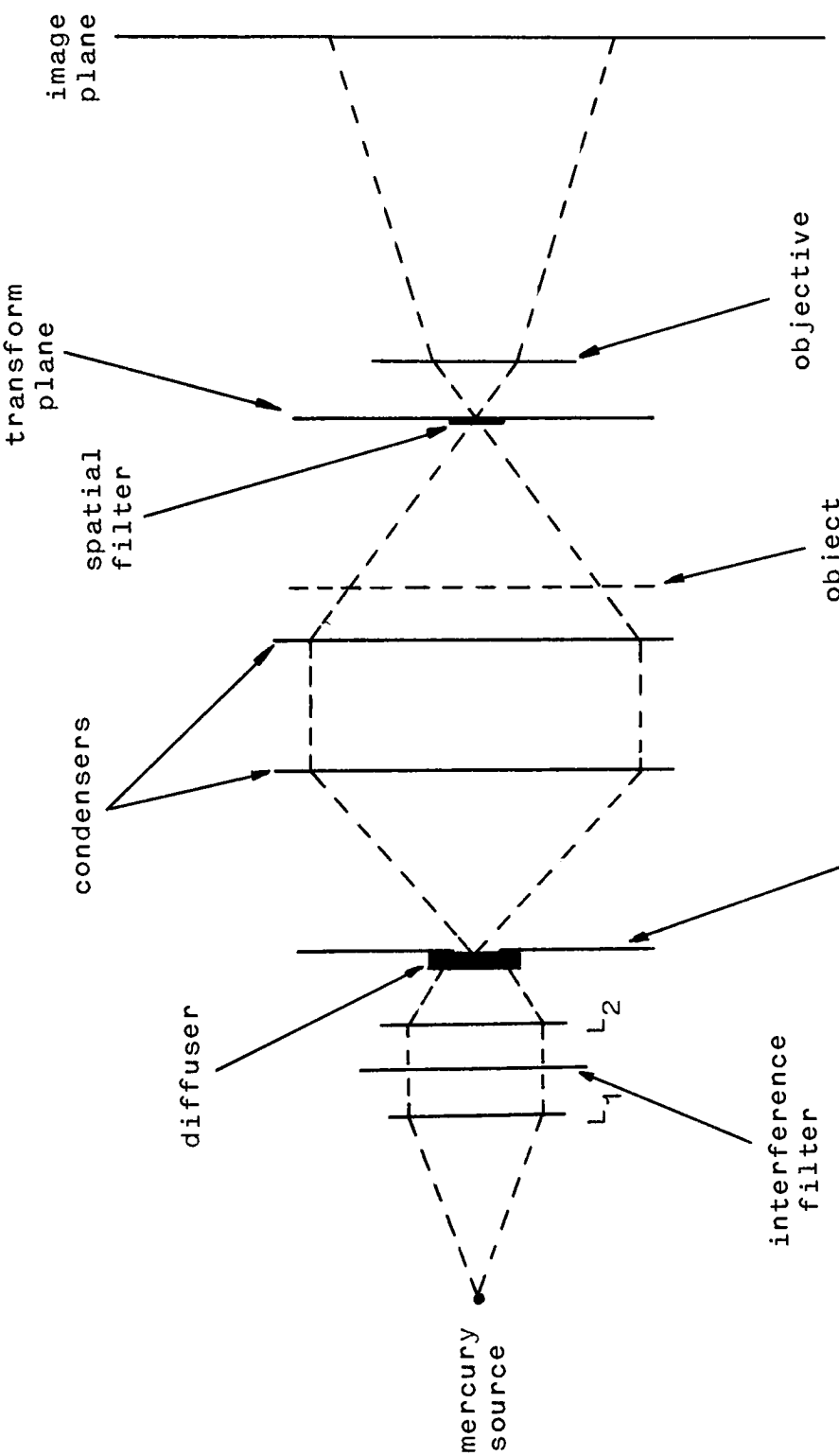

Optical Schematic

figure 7

where r=distance from first condenser
a=source diameter
λ=average wavelength

$$v = \frac{3.83(65mm)(.000436mm)}{2\pi(3mm)}$$

$$\cong .0058 \text{ mm}$$

The value of .011 mm was found by Radl to produce incoherent imaging properties, such as maximum resolution and minimum sharpness when using a similar optical geometry. An estimated coherence interval of .0058 mm shows increased incoherence over Radl's experimental work, but will still produce similar imaging properties.

The condensers used were two Wollensak Raptar 152 mm f/2.8 aerial lenses used back to back. These optics provide maximum performance when a long conjugate is used on the object side, and using them as a pair retained these properties. Spacing between the condensers was approximately 235 mm, which produced a source image at a magnification of 1.0 located 160 mm from the second condenser. A Komura 135 mm f/5.6 enlarging lens was used as an objective, and was positioned so the source image was approximately 2 mm from the rear element of the objective. This source image is also the location of the transform plane, which lent it to spatial filtering. The transmission object was located 16 mm from the rear element of the second condenser which provided an image

with a magnification of 5.3.

The theoretical cutoff frequencies for both incoherent and coherent imaging systems can be predicted to first order with the following expressions.

$$\text{incoherent cutoff } v_{inc} = \frac{1}{\lambda N_{eff}}$$

$$v_{inc} = \frac{1}{.000436\text{mm}(35)} \cong 65 \text{ cyc/mm}$$

$$\text{coherent cutoff } v_{coh} = \frac{1}{2\lambda N_{eff}}$$

$$\cong 32 \text{ cyc/mm}$$

where N_{eff}= effective f/number

$$N_{eff} = N(1+MAG) = 5.6(1+5.3)$$

$$N_{eff} \cong 35$$

Refering to figure 1, the distance between frequency values f_1 and f_0 can also be estimated to first order knowing the wavelength of the quasi-monochromatic illumination and the distance s from the last element of the second condenser to the transform plane. Using this value, the cutoff frequency

$$\frac{1}{\lambda s}(\text{cyc/mm-mm}) = \frac{1}{(.000436\text{mm})(160\text{mm})}$$

$$= 14 \text{ cyc/mm-mm}$$

for various filters may be found by multiplying a given filter radius by the above conversion factor. Table 1 lists the approximate cutoff frequencies in the Fourier transform plane of the filters used.

Table 1

Filter Cutoff Frequencies

filter radius	cutoff frequency
.3mm	4.2cyc/mm
1.1	15.4
1.5	21.0

A test object was produced by contact printing a high contrast tri-bar resolution target imaged on a glass plate onto 35mm Kodak Fine Grain Positive Release Film and processed in Kodak D-76 developer. The resolution test object was produced having a transmission modulation of approximately .5. A pre-exposure fog was first given to obtain the necessary transmission values for a modulation of .5.

With a source diameter of 3.0 mm, spatial filter diameters of .6, 2.2, and 3.0 mm were chosen as a representative range. Filters were constructed by first drilling holes at the above diameters halfway through 2 inch plexiglass squares, measuring their diameter on a measuring microscope. The holes were then filled with black paint, and the opaque plexi-glass filters were contact printed onto Kodak Kodalith high contrast film, which resulted in a mask of spatial filters. This mask was contact printed onto Kodak

Fine Grain Positive Release Film to produce spatial filters of a density of approximately 1.0. Fine Grain Positive film was chosen because of its low base plus fog density which transmitted the maximum amount of energy in the high frequency range, while the thin emulsion would minimize the phase shift encountered due to an increased optical path length when passing through the emulsion of the filtered region.

Images of the .5 modulation resolution target were made onto Fine Grain Positive film, using a 35mm camera back as a film plane. Test images were produced without a spatial filter, and with each of the filters having diameters of .6, 2.2, and 3.0 mm. Resolving power test images were viewed under 60X magnification by 5 trained observers to determine the affect of spatial filtering on resolving power. Sensitometric exposures were made and processed with all test images. Exposures between all test images were within 10 percent.

A Joyce-Lobel scanning microdensitometer was used to evaluate the images. Edge information present in the resolution target allowed edge gradient analysis and resolution data to be obtained from one test target. The .5 modulation target had a D_{min} of .10, and a D_{max} equal to .61, which is a medium contrast target with which all analysis was done. All targets were scanned with the effective slit dimensions of .01mm X .23mm.

Test prints were made of the resolution test images

at a magnification of 15X, and are located in appendix A, figure A-1. A pictorial scene was also photographed on Kodak Tri-X pan film and imaged with the unfiltered projection system. The image was then printed using the 2.2 mm spatial filter and conclusions were drawn. Prints were evaluated by inspection for overall sharpness to determine the affect of spatial filtering on subjective image quality.

RESULTS

As mentioned previously, all edge images were scanned on a Joyce-Lobel recording microdensitometer, and density profiles were obtained. The edges were sampled at intervals such that sixteen samples were obtained. These density values were converted to effective exposure by tracing them back through the density versus relative log exposure curve. Normalized irradiance values were then plotted as a function of distance along the sampled edge and are illustrated in figure 8. It can be seen that increased ringing occured in the edge images, which appears as normalized irradiance values greater than 1, as the mathematical model predicted. The number in parenthesis indicates the diameter of the filter in millimeters used with the 3 mm source. An edge gradient value was not assigned to this data as a descriptor due to the increasing assymetry of the curves. By inspection, the edge gradient, as determined by the slope of the linear portion of the curve, would be nearly invariant despite the grossly changing shape of the edge irradiance functions.

The unfiltered case (0) produced an edge with no ringing, the steepest apparent edge gradient, and essentially no toe portion to the irradiance curve. As the filter size increased to (.6), (2.2), and (3.0), an increase in both the

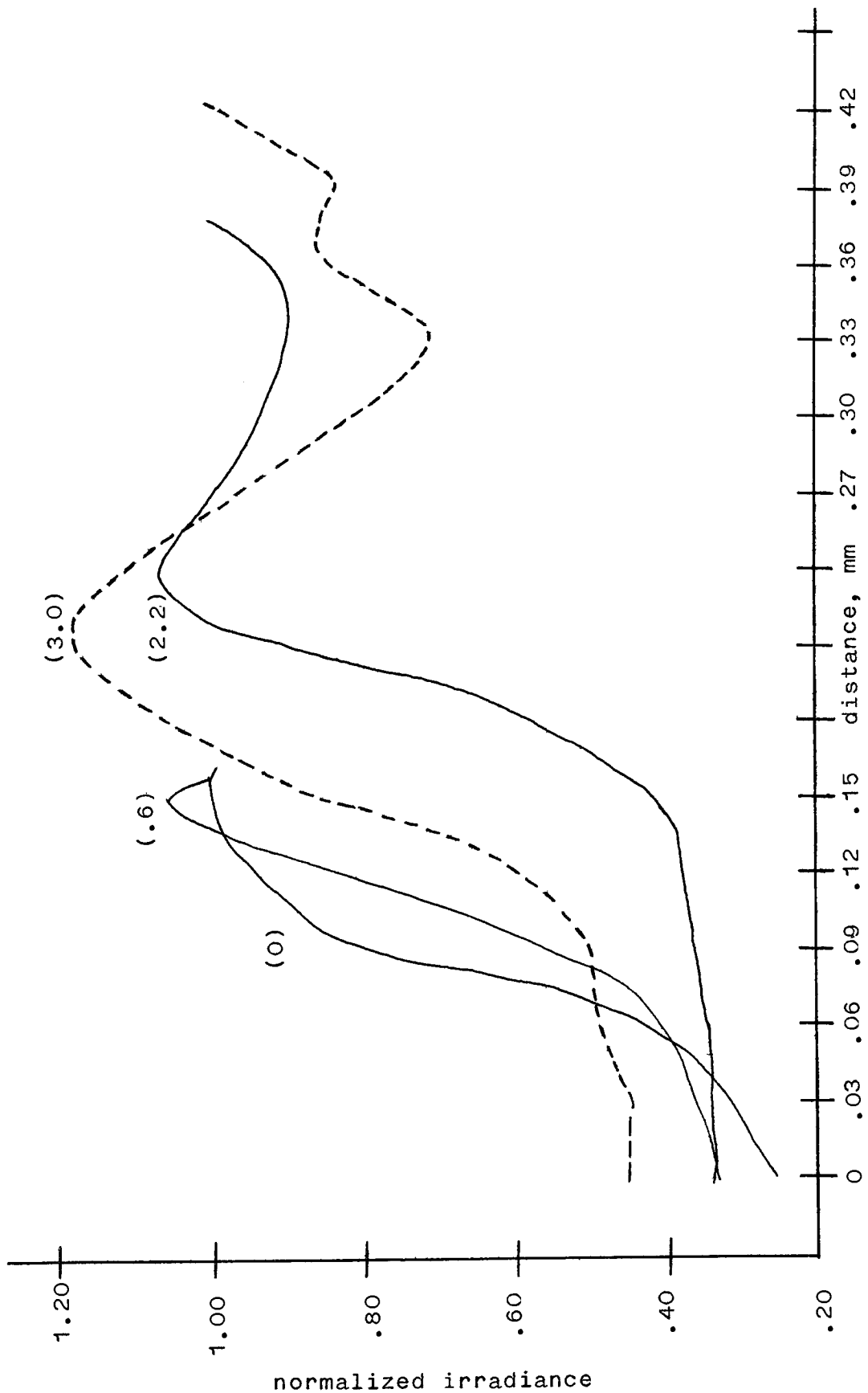

Edge Traces
figure 8

length of the toe portion of the curve and the amount of ringing present in the images is evident.

The modulation transfer function was determined by differentiating normalized edge irradiance values and using a sixteen point Cooley-Tukey Fast Fourier Transform stored as a Fortran subroutine in the Xerox Sigma 9 computing system at RIT. The affect of spatial filtering on MTF is illustrated by figure 9. The cutoff frequency for the unfiltered case is found to be approximately 49 cyc/mm. This value is in reasonable agreement with the previously determined theoretical incoherent and coherent cutoff frequencies of 65 cyc/mm and 32 cyc/mm respectively. The intermediate experimental cutoff frequency of 49 cyc/mm is a reasonable estimate for this partially coherent imaging system. Resolving power was subjectively found to be 14 cyc/mm.

Applying the .6 mm spatial filter to the system results in a cutoff frequency of approximately 41 cyc/mm, or a decrease of 16 percent. Modulation values were found to be lower across all frequencies. This is visually evident on images of the test targets located in appendix A, figure A-1. Overall modulation for the test image (.6) is seen to have decreased. Ringing in the image of the tri-bar target can also be detected, causing resolving power to drop to 11 cyc/mm.

Spatial filtering with the 2.2 mm filter resulted in a cutoff frequency of 20 cyc/mm, representing a decrease

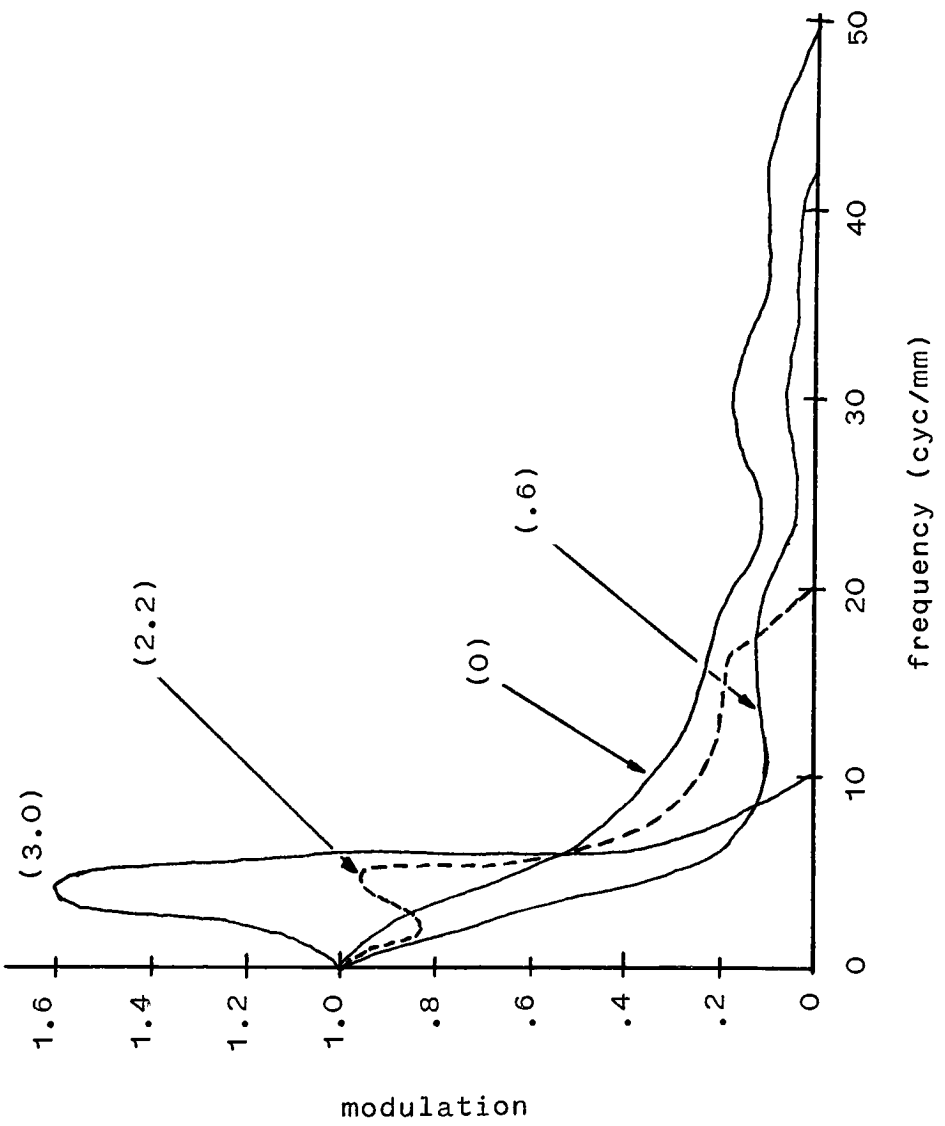

MTF curves
figure 9

of 60 percent. Modulation was found to have increased in the range from 3 cyc/mm to 6 cyc/mm by about 30 percent. Looking at the test print in figure A-1 of (2.2), a slight increase in modulation can be seen over other cases previously mentioned. Resolving power was determined to be 12 cyc/mm, an increase of 1 element over the image filtered with the .6 mm filter.

Pictorial prints, figure A-2, were made with the (2.2) filter, and it was determined that no significant change in image quality was attained with the spatial filtering technique. The two photographs are indistinguishable when imaged with the optical geometry described.

Attenuating the entire source diameter caused a phase reversal in the image, which is evident in figure A-1, (3.0). The MTF of this system yielded a cutoff frequency of approximately 10 cyc/mm. Severe ringing is encountered in this case as seen in the normalized irradiance versus distance plot, figure 7, which results in normalized irradiance values greater than one. Values of modulation are also in excess of one in the frequency range 0-6 cyc/mm. Difficulty in reading the resolution target made resolution values meaningless, and therefore are not reported.

CONCLUSIONS

Spatial filtering has been seen to have a drastic affect on image quality parameters such as edge gradient, and the modulation transfer function. Resolution, however, has been found to be a poor descriptor of this imaging system. A 60 percent decrease in cutoff frequency, and varying intermediate values of modulation caused only a 10 percent decrease in resolving power by inspection of the data of the unfiltered system and that of the system filtered with the 2.2 mm oclusion. The general trend has been a decrease in cutoff frequency and an increase in low frequency modulation with the use of spatial filtering.

Subjectively, however, the use of spatial filtering was found to have no significant affect on image quality at the 5.3X magnification used. Any changes in image quality should have been noticed at low magnifications due to the increased low frequency modulation. It is therefore concluded that with the system geometry and illumination characteristics used, the magnitude of change of projection characteristics is too small to be detected visually.

REFERENCES

REFERENCES

1 J.W. Goodman, Introduction to Fourier Optics, (McGraw Hill Co., 1968) p. 142.

2 R.A. Phillips, American Journal of Physics, 37, 536(1969).

3 E. Hecht and A. Zajac, Optics, (Addison-Wesley Publishing Co., Reading,Mass., 1976) pp.424-426.

4 D. Grimes and B. Thompson, Journal of the Optical Society of America, 57, 1330(1967).

5 B. Radl, Image Quality Dependence on Partial Coherence in a Projection Printer, (RIT, 1979).

6 R. Kinzly, Journal of the Optical Society of America, 55, 1002(1965).

APPENDIX

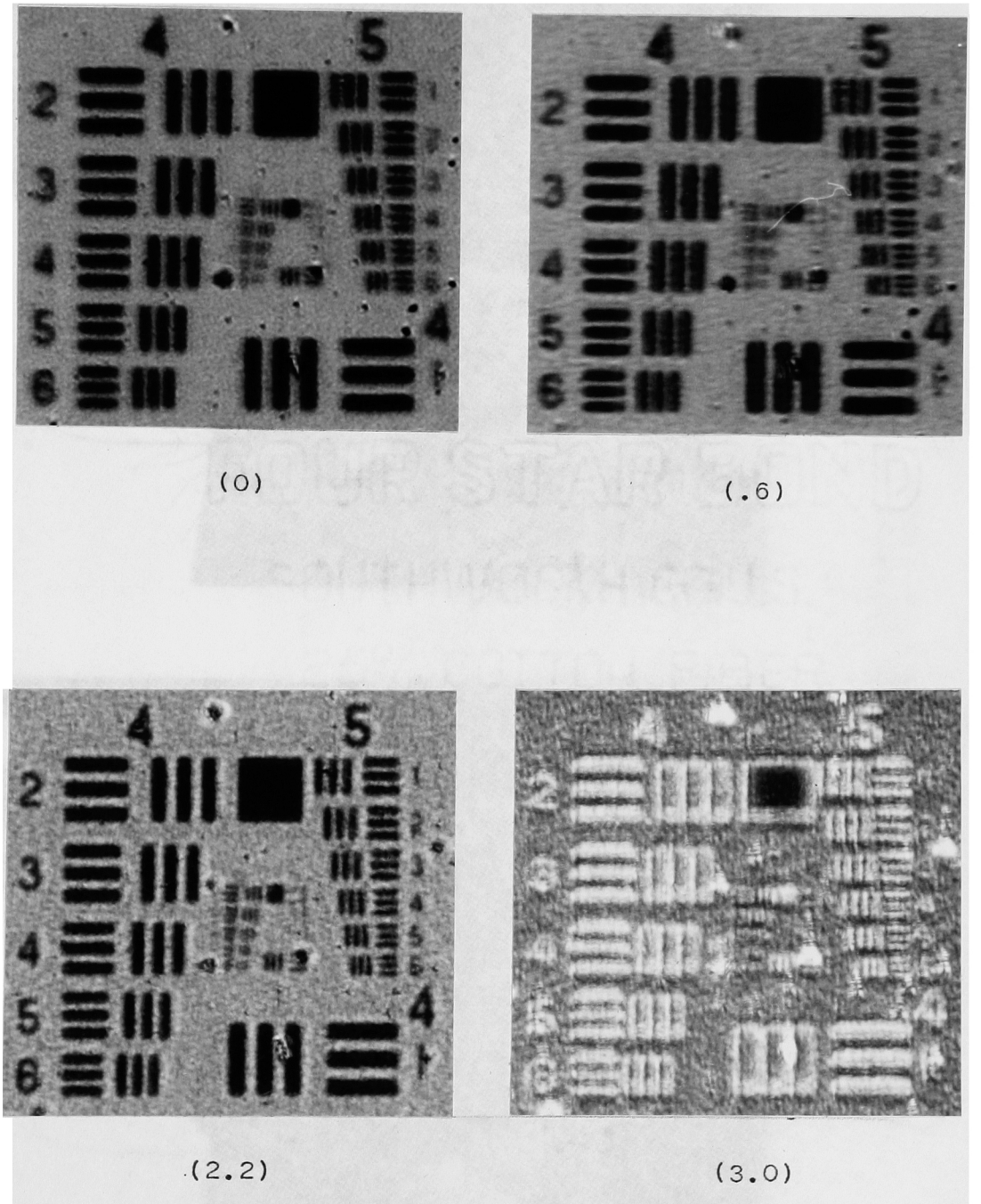

Spatially Filtered Images (mm)

figure A-1

A B

Unfiltered (A) and Filtered (B) Images
Using 2.2 mm Filter

figure A-2